

## Kinase Pathway Dependence in Primary Human Leukemias Determined by Rapid Inhibitor Screening

Jeffrey W. Tyner<sup>1,3</sup>, Wayne F. Yang<sup>3,4</sup>, Armand Bankhead III<sup>5</sup>, Guang Fan<sup>2</sup>, Luke B. Fletcher<sup>3,4</sup>, Jade Bryant<sup>3,4</sup>, Jason M. Glover<sup>3,6</sup>, Bill H. Chang<sup>3,6</sup>, Stephen E. Spurgeon<sup>3,4</sup>, William H. Fleming<sup>3,4,7</sup>, Tibor Kovacsovics<sup>3,4</sup>, Jason R. Gotlib<sup>9</sup>, Stephen T. Oh<sup>10</sup>, Michael W. Deininger<sup>11</sup>, Christian Michel Zwaan<sup>12,13</sup>, Monique L. Den Boer<sup>12</sup>, Marry M. van den Heuvel-Eibrink<sup>12</sup>, Thomas O'Hare<sup>11</sup>, Brian J. Druker<sup>3,4,8</sup>, and Marc M. Loriaux<sup>2,3,4</sup>

### Abstract

Kinases are dysregulated in most cancers, but the frequency of specific kinase mutations is low, indicating a complex etiology in kinase dysregulation. Here, we report a strategy to rapidly identify functionally important kinase targets, irrespective of the etiology of kinase pathway dysregulation, ultimately enabling a correlation of patient genetic profiles to clinically effective kinase inhibitors. Our methodology assessed the sensitivity of primary leukemia patient samples to a panel of 66 small-molecule kinase inhibitors over 3 days. Screening of 151 leukemia patient samples revealed a wide diversity of drug sensitivities, with 70% of the clinical specimens exhibiting hypersensitivity to one or more drugs. From this data set, we developed an algorithm to predict kinase pathway dependence based on analysis of inhibitor sensitivity patterns. Applying this algorithm correctly identified pathway dependence in proof-of-principle specimens with known oncogenes, including a rare FLT3 mutation outside regions covered by standard molecular diagnostic tests. Interrogation of all 151 patient specimens with this algorithm identified a diversity of kinase targets and signaling pathways that could aid prioritization of deep sequencing data sets, permitting a cumulative analysis to understand kinase pathway dependence within leukemia subsets. In a proof-of-principle case, we showed that *in vitro* drug sensitivity could predict both a clinical response and the development of drug resistance. Taken together, our results suggested that drug target scores derived from a comprehensive kinase inhibitor panel could predict pathway dependence in cancer cells while simultaneously identifying potential therapeutic options. *Cancer Res*; 73(1); 285–96. ©2012 AACR.

### Introduction

Gene-targeted cancer therapies have achieved remarkable clinical outcomes in recent years (1–4). In particular, cell-permeable small molecules that exhibit inhibitory activity against tyrosine kinases have generated great interest. Tyrosine kinases represent a gene family widely implicated in

cancer pathogenesis (5, 6), and dysregulation of specific tyrosine kinases has been observed in most hematologic malignancies, including chronic myeloid leukemia (CML; ref. 7), chronic myelomonocytic leukemia (CMML; refs. 8–11), other myeloproliferative neoplasms (MPN; refs. 12–15), acute myeloid leukemia (AML; refs. 9, 16–20), acute lymphoblastic leukemia (ALL; refs. 21–26), and chronic lymphocytic leukemia (CLL; refs. 27–30). Although a minority of patients with hematologic malignancies are successfully treated with kinase inhibitors, most patients remain ineligible for this form of targeted therapy due to lack of knowledge of the specific kinase pathways involved.

Many strategies exist to better understand kinase dysregulation in cancer including the recent development of deep sequencing techniques, which are accelerating our understanding of cancer genetics. Thus far, however, many studies of malignancies with predicted kinase pathway dependence have not found frequent mutations in kinase genes (31–34). These findings suggest that kinase pathway dependence in malignant cells often occurs due to complex genetic mechanisms. Hence, although deep sequencing represents an immensely powerful technique, it may not independently allow for prediction of kinase targets and kinase inhibitor therapies. Instead, understanding of the best kinase inhibitor therapies for patients will likely require the combination of deep sequencing with complementary studies that can define kinase

**Authors' Affiliations:** <sup>1</sup>Departments of Cell and Developmental Biology and <sup>2</sup>Pathology; <sup>3</sup>Knight Cancer Institute; Divisions of <sup>4</sup>Hematology and Medical Oncology and <sup>5</sup>Bioinformatics and Computational Biology; <sup>6</sup>Division of Pediatric Hematology and Oncology and <sup>7</sup>Stem Cell Center, Department of Pediatrics, Oregon Health & Science University; <sup>8</sup>Howard Hughes Medical Institute, Portland, Oregon; <sup>9</sup>Stanford Cancer Center, Stanford University School of Medicine, Stanford, California; <sup>10</sup>Department of Medicine, Hematology Division, Washington University School of Medicine, Washington University in St. Louis, St. Louis, Missouri; <sup>11</sup>Department of Internal Medicine, Huntsman Cancer Institute, University of Utah, Salt Lake City, Utah; <sup>12</sup>Department of Pediatric Hematology/Oncology, Erasmus Medical Center/Sophia Children's Hospital, Rotterdam; and <sup>13</sup>Dutch Childhood Oncology Group, Den Haag, the Netherlands

**Note:** Supplementary data for this article are available at Cancer Research Online (<http://cancerres.aacrjournals.org/>).

**Corresponding Author:** Marc M. Loriaux, Department of Pathology, OHSU BRB 553, Mailcode L592, 3181 SW Sam Jackson Park Road, Portland, OR 97239. Phone: 503-494-9893; Fax: 503-494-3688; E-mail: [loriauxm@ohsu.edu](mailto:loriauxm@ohsu.edu)

doi: 10.1158/0008-5472.CAN-12-1906

©2012 American Association for Cancer Research.

targets regardless of mutational status. These functionally important kinase pathways can then be correlated with genetic profiles that have been revealed by deep sequencing.

To better define the use of kinase inhibitor therapies in hematologic malignancies, we have developed a small-molecule kinase inhibitor panel designed to identify kinase pathway dependence in primary leukemia samples. To analyze kinase pathway dependence based on this functional data, we have developed an accompanying bioinformatics approach to predict the kinase targets underlying inhibitor sensitivity profiles. This algorithm takes advantage of our knowledge of the gene products that are targeted by each drug as well as the fact that these target profiles are partially overlapping. Using the overlap of effective drugs and eliminating targets of ineffective drugs, we are able to predict critical kinase targets and signaling pathways for individual patient samples. These kinase target predictions represent a manner by which functional data from drug screening could be integrated with genomics data such as deep sequencing to aid in prioritization of sequence variants and, thus, accelerate our understanding of molecular etiologies of cancer as well as application of individualized therapeutic approaches for patients.

## Materials and Methods

### Kinase inhibitors

Kinase inhibitors were purchased from or were generously provided by the sources outlined in Supplementary Table S7.

### Collection of patient samples and cell culture

All clinical samples were obtained with informed consent with approval by the Institutional Review Boards of Stanford University (Stanford, CA), Oregon Health & Science University (Portland, OR), the Children's Oncology Group, and Erasmus Medical Center/Sophia Children's Hospital (Rotterdam, the Netherlands). Blood or bone marrow from patients was separated on a Ficoll gradient and mononuclear cells were treated with ammonium-chloride-potassium (ACK) lysis buffer. The only exceptions to this procedure were cases of atypical CML or chronic neutrophilic leukemia, where samples were only processed with ACK lysis buffer to preserve the neoplastic granulocytes that would otherwise be lost on the Ficoll gradient. Cells from myeloid leukemia samples were cultured in R10 [RPMI-1640 medium supplemented with 10% FBS (Atlanta Biologicals), L-glutamine, penicillin/streptomycin (Invitrogen), and fungizone (Invitrogen)] supplemented with  $10^{-4}$  M 2-mercaptoethanol (Sigma). Cells from lymphoid leukemia samples were cultured in R20 [RPMI-1640 medium supplemented with 20% FBS (Atlanta Biologicals), L-glutamine, penicillin/streptomycin (Invitrogen), and fungizone (Invitrogen)] supplemented with  $10^{-4}$  M 2-mercaptoethanol (Sigma) insulin-transferrin-sodium selenite (Invitrogen).

### Kinase inhibitor screen

Kinase inhibitors were stored at 10 to 100 mmol/L in dimethyl sulfoxide (DMSO; stock concentration was 1,000 times the final concentration of the highest tested dose). Drugs were used at final concentrations shown in Supplementary Table S4. For creation of replicate plates of the library, each

drug concentration was diluted to twice the final concentration and 50  $\mu$ L were plated into 96-well plates using a Hydra 96-channel automated pipettor (Matrix Technologies). Plates were sealed with adhesive lids (Bio-Rad; microplate seal B), wrapped in aluminum foil, and stored at  $-20^{\circ}\text{C}$  until use. Upon receipt of a patient sample, plates were thawed at  $37^{\circ}\text{C}$ , 5%  $\text{CO}_2$  for 1 hour and centrifuged at  $800 \times g$  before removal of adhesive lids. Subsequently, patient samples were suspended into culture media at a concentration of 1,000,000 cells per mL, such that addition of 50  $\mu$ L to each well would deliver 50,000 cells to that well (this also dilutes the drugs to their final, desired concentration). Cells were incubated for 3 days at  $37^{\circ}\text{C}$ , 5%  $\text{CO}_2$  and subjected to a CellTiter 96 AQueous One solution cell proliferation assay (Promega). Each plate contained 7 wells without any drug. The average absorbance value of these 7 wells was used for data normalization and the kill curve of each drug gradient was assessed relative to this average no-drug point.

### Quantification of patient response and effective drug targets

An algorithm was designed and implemented using Excel and Visual Basic to provide automated  $\text{IC}_{50}$  calculation and therapeutic target identification.  $\text{IC}_{50}$  values were calculated using second-degree polynomial regression curves fit through 5 data points (average of no drug wells and 4 serial dilution points). All curves were manually inspected and a small number of  $\text{IC}_{50}$ s were corrected in 2 circumstances: (1) The curve fit intersected the  $\text{IC}_{50}$  at 2 distinct points—the lower concentration intersect was used in these instances; (2) the polynomial curve fit yielded an artificial  $\text{IC}_{50}$  not reflected in the data points (generally due to increasing cell viability over the course of the drug titration). For a given sample, drug  $\text{IC}_{50}$  values were considered effective if they were less than or equal to 5-fold below the median  $\text{IC}_{50}$  for all samples tested. Where an  $\text{IC}_{50}$  was not achieved for a given drug, an  $\text{IC}_{50}$  value equal to the highest drug concentration used was arbitrarily assigned. After effective and ineffective drugs were determined for each sample, a drug target score was assigned by the program for each potential therapeutic target.

The drug target score is based on the  $\text{IC}_{50}$  measured effectiveness of panel drugs against a given therapeutic target for a given patient. Each drug is associated with a "tiered" ranking of target kinases for which the drug has been shown to biochemically associate (35, 37–43). Weights are used to give a stronger quantitative emphasis to targets with a higher ranking (Figs. 4A and 4C). Scores are determined empirically for a given sample by assigning positive weighted scores to targets of effective drugs and negative weighted scores to targets of ineffective drugs. Drug effectiveness threshold and tiered ranking weights were determined empirically using patient samples and cell lines with known kinase signaling abnormalities. The algorithm generates a cumulative drug target score for each target according to the following equations:

$$\text{Effective drug target score} = \sum_{i=1}^n \text{Weight}_{\text{Tier}}(i)$$

Where  $\text{Weight}_{\text{Tier}}(i)$  is a given drug target's tier ranking for drug  $i$  and  $n$  is the number of effective drugs.

And

$$\text{Ineffective drug target score} = \sum_{j=1}^m \text{Weight}_{\text{Tier}}(j)$$

Where  $\text{Weight}_{\text{Tier}}(j)$  is a given drug target's tier ranking for drug  $j$  and  $m$  is the number of ineffective drugs.

$$n + m = 66.$$

Final drug target score = effective drug target score + ineffective drug target score

Hierarchical clustering was conducted using GenePattern software (Broad Institute). Sample clustering and 2-way clustering by row (drug) and column (patient sample) were conducted using Pearson correlation distance shown in Fig. 6 and Supplementary Figs. S2 and S3.

## Results

### Development of a kinase inhibitor panel for analysis of primary leukemia specimens

The ubiquitous role of tyrosine kinases in regulating critical cellular processes leading to malignancy suggests that a large percentage of leukemia (and other malignancy) patient samples would exhibit sensitivity to inhibition of one or more kinase pathways. To test this hypothesis, we compiled a library of 66 small-molecule kinase inhibitors with collective activity against two-thirds of the tyrosine kinome (Supplementary Table S1). Because many nontyrosine kinases are also critical regulators of cellular growth/survival, we also included drugs with activity against select families of nontyrosine kinases including phosphoinositide-3 kinase (PI3K)/AKT, PKC, PKA, IKK, RAF/MEK/ERK, *c-jun*-NH2-kinase (JNK), p38, AMPK, aurora kinases, and cyclin-dependent kinases (Supplementary Table S1). Each inhibitor was plated at 4 graded concentrations that bracket the predicted on-target  $\text{IC}_{50}$  value. Primary patient samples were incubated with this panel of drugs for 3 days at which point a tetrazolium-based cell viability assay (MTS) was conducted for assessment of cell viability. All values were normalized to cells incubated in the absence of drug (Supplementary Fig. S1).

### Analysis of 151 leukemia patient samples with small-molecule kinase inhibitor panel

Over a 2-year period, we accrued and tested 151 fresh, primary leukemia patient samples against this panel of kinase inhibitors. The cohort was comprised of 34 AML, 42 ALL, 31 MPN, and 44 CLL patients. Detailed clinical and demographic information about this patient cohort can be found in Supplementary Table S2. Assessment of kinase inhibitor hypersensitivity profiles of these 151 leukemia patient samples revealed a wide diversity of responses to kinase inhibitors, even when patients were grouped according to diagnostic subsets and kinase inhibitors grouped according to predicted kinase target spectra (Fig. 1). Despite this heterogeneity of responses, certain trends emerged, such as more frequent sensitivity to PI3K/AKT inhibitors in lymphoid samples. In addition, select cases could be identified with universal sensitivity to whole families of kinase inhibitors. For example, AML case 07335 exhibited universal sensitivity to all ERBB

family inhibitors on the panel, suggesting involvement of an ERBB family member in maintenance of the viability of malignant cells from that patient (Fig. 1). Overall, 70% of patients exhibited hypersensitivity to one or more kinase inhibitors ( $\text{IC}_{50}$  data for each drug for each patient specimen listed in Supplementary Table S3; raw data points used to generate these  $\text{IC}_{50}$ s listed in Supplementary Table S4). Nine of the drugs on our panel are currently approved by the U.S. Food and Drug Administration (FDA; imatinib, nilotinib, dasatinib, sunitinib, erlotinib, gefitinib, lapatinib, sorafenib, and pazopanib), and approximately 40% of samples exhibit hypersensitivity to one or more of these 9 drugs. Hypersensitivity to a drug was determined by comparison of the response of each individual sample with the response of all other samples (patient  $\text{IC}_{50}$  compared with whole cohort median  $\text{IC}_{50}$ ). In this way, we could define outlier samples that were truly hypersensitive to a given drug versus responses at higher concentrations that might occur due to off-target toxicity of the compound. Rank ordering of patient  $\text{IC}_{50}$ s for each drug helps illustrate this point (Supplementary Fig. S2). To better distinguish inhibitor sensitivity profiles that were similar from patient to patient, we applied one-way Pearson correlation for hierarchical clustering of the data (Supplementary Fig. S3). Notably, although drug responses are clearly not uniform among diagnostic subsets, there were large groups of patients diagnosed with the same type of leukemia [notably ALL (shaded red) and CLL (shaded yellow); Supplementary Fig. S3] with similar responses to these kinase inhibitors. However, the segregation of sample responses by cell type was far from complete with a number of isolated lymphoid samples clustering amidst myeloid cases and vice versa. In addition, 2-way hierarchical clustering revealed drugs with similar activity profiles across patients (Supplementary Fig. S4). Many of these drugs clustered in groups that would be predicted on the basis of known target profiles of the compounds such as BIRB-796 and VX-745 (both p38 inhibitors), flavopiridol and BMS-387032 (both CDK inhibitors), and EKB-569 and CI-1033 (both ERBB-family inhibitors).

### Logical prediction of oncogenic signaling pathways using inhibitor sensitivity profiles

Clinical and research interest in the application of kinase inhibitors has led to a concerted effort to develop techniques that characterize the targets to which each compound can effectively bind (35–38). Because a majority of the kinase inhibitors on our panel have been characterized in this manner, we realized that this information could be used to predict the critical kinase targets and signaling pathways that underlie the observed kinase inhibitor sensitivity patterns. Development of this bioinformatics approach relies on the fact that all kinase inhibitors on our panel bind multiple targets and the target spectra for these drugs are partially overlapping. Thus, if a sample exhibits sensitivity to 2 different drugs, the kinase targets that are commonly inhibited by both drugs are implicated as most likely to explain this sensitivity pattern (unless there are 2 different pathways operational in that sample). A second step can further narrow the candidate kinase list



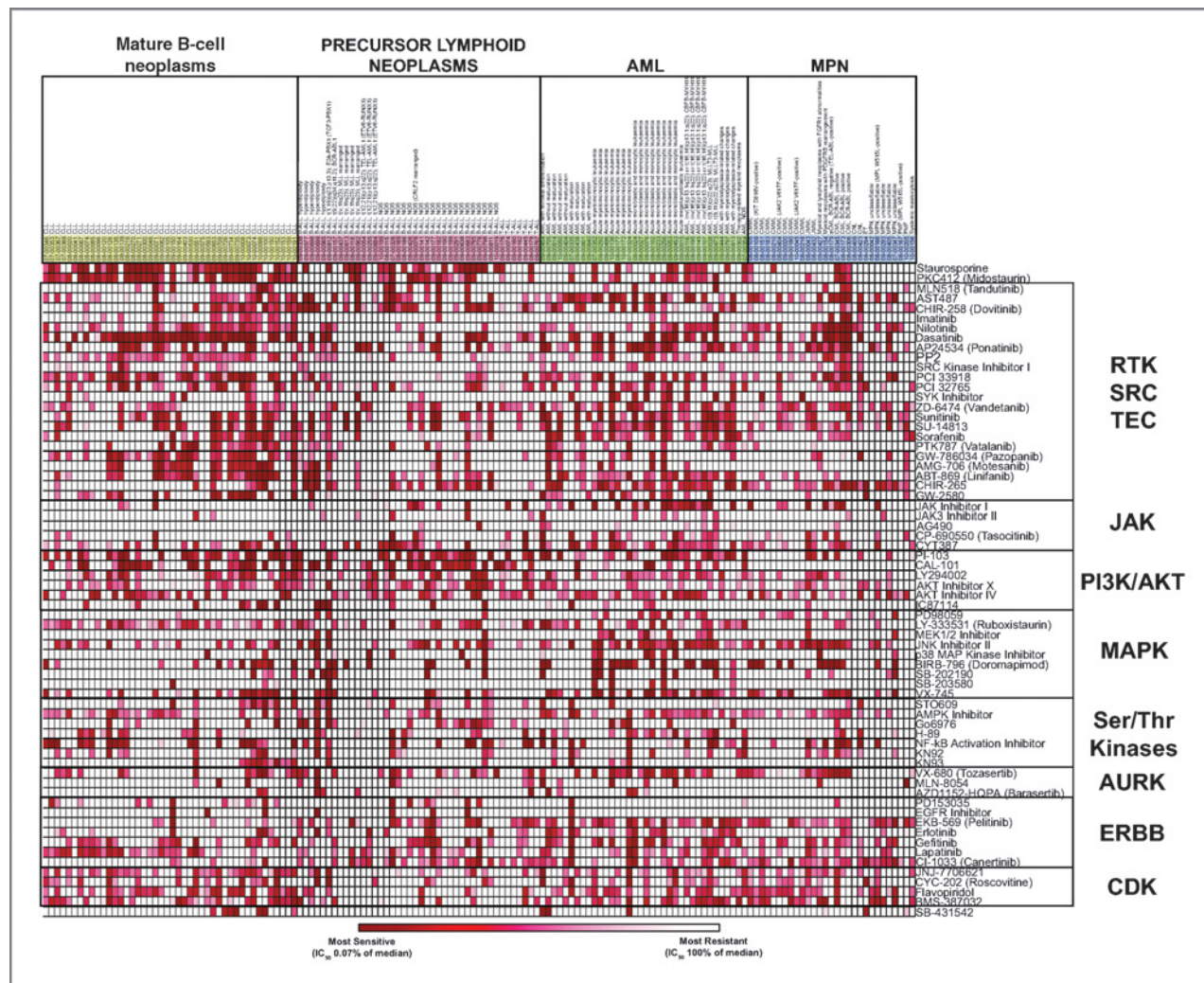


Figure 1. Response of 151 leukemia patient samples to 66 small-molecule kinase inhibitors. Mononuclear cells were obtained from 151 primary leukemia patient samples and IC<sub>50</sub> values for 66 small-molecule kinase inhibitors were tabulated as described in Supplementary Fig. S1. The percentage of median IC<sub>50</sub> for each patient for every drug is expressed on this heatmap where darkest red indicates most sensitive (most sensitive patient sample to any drug was 0.07% of median) and white indicates completely insensitive (IC<sub>50</sub> for patient is at or above 100% of median). Patient samples are arranged by diagnosis (ALL, red; AML, green; CLL, yellow; MPN, blue). Kinase inhibitors are arranged on the basis of family of primary kinase targets for each drug. Numerical input for this heatmap is found in Supplementary Table S3.

by elimination of targets of drugs to which a sample is not sensitive.

The results from AML patient 08024 illustrate our target identification strategy. Malignant cells from this patient were hypersensitive to 3 drugs: AST-487, sunitinib, and SU-14813. As noted above, drug hypersensitivity is defined by comparison of the IC<sub>50</sub> values for this individual sample with the median IC<sub>50</sub> values that these drugs achieved across the entire cohort. Cells from patient 08024 exhibited IC<sub>50</sub> values that were at least 5-fold lower than the cohort median IC<sub>50</sub> values for each of these 3 drugs (Fig. 2A). Analysis of the known targets of these 3 compounds revealed 4 kinases, KIT, PDGFR, CSF1R, and FLT3, that are common targets between all 3 drugs (Fig. 2B). Because this sample was also unaffected by the 2 drugs, dasatinib and nilotinib (no difference between patient 08024 IC<sub>50</sub> and median IC<sub>50</sub>; Fig. 2A), the kinase targets of these 2

drugs can be eliminated from consideration as kinases that could mechanistically explain cell viability in this patient sample. The kinase targets that are effectively inhibited by dasatinib and/or nilotinib are shaded blue, whereas the kinases not targeted by either dasatinib or nilotinib are shaded red (Fig. 2B). This reveals that the only kinase target in common between AST-487, sunitinib, and SU-14813 that is also not a target of dasatinib or nilotinib is FLT3. Further analysis of AML patient 08024 revealed presence of the *FLT3-ITD* and no wild-type *FLT3* alleles (Fig. 2C).

#### Development of a customized algorithm to automate oncogenic pathway prediction

Application of the logic illustrated in Fig. 2B can be conducted manually for a small number of kinase inhibitors; however, expansion of this process to evaluate data from the

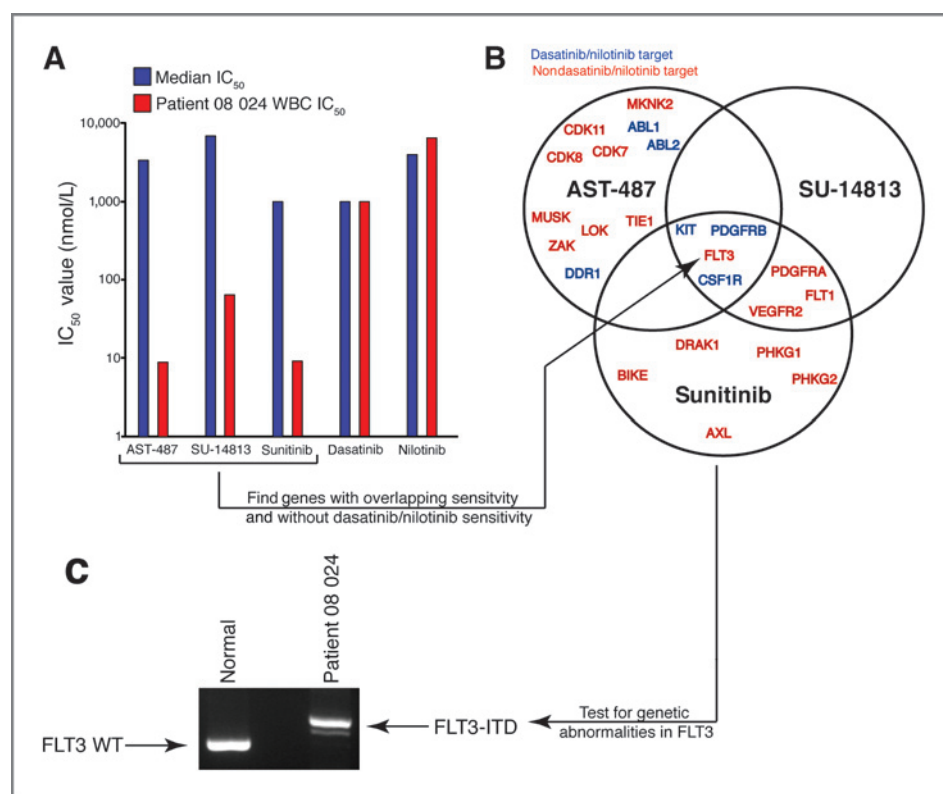


**Figure 2.** Logical prediction of kinase targets based on drug sensitivity/resistance. To predict operational kinase targets in Patient 08024, response to 5 kinase inhibitors was considered. A, patient 08024 exhibited at least 5-fold lower  $IC_{50}$  than median to AST-487, SU-14813, and sunitinib (effective drugs), whereas no difference is seen between median and patient 08024  $IC_{50}$ s for dasatinib and nilotinib (ineffective drugs). To predict targets that underlie this sensitivity pattern, the overlap of kinase targets between the 3 effective drugs (AST-487, SU-14813, and sunitinib) is shown in B revealing that only KIT, PDGFR, CSF1R, and FLT3 are common kinase targets between these drugs. To distinguish between these 4 targets, their responsiveness to the ineffective drugs (dasatinib and nilotinib) was considered. The kinase targets in blue (KIT, PDGFR, CSF1R) are good targets of dasatinib and/or nilotinib, whereas the kinase targets in red (FLT3) were not effectively inhibited by dasatinib or nilotinib. Elimination of these dasatinib/nilotinib targets (in blue) leaves only FLT3 as a potential kinase target for explanation of the functional response to these 5 drugs. Follow-up PCR analysis revealed this AML patient sample to exhibit FLT3-ITD with loss of the wild-type FLT3 allele (C).

entire panel of 66 drugs requires computational support. We have developed an algorithm to carry out the same logical steps outlined in Fig. 2, for all 66 kinase inhibitors in 4 steps (Sweave document with instructions for generating application to perform this algorithm can be found in Supplementary Material). First, the kinase target information for each drug was curated from published sources (35, 37–43) into a database (Fig. 3A and Supplementary Table 1). Second, the  $K_d$  or  $IC_{50}$  values (depending on the format of assay used to define drug targets) for each drug were subdivided into 5 tiers on a  $\log_{10}$  scale. The first tier is defined as the kinase with the lowest  $K_d$  or  $IC_{50}$  value as well as all other kinases with  $K_d$  or  $IC_{50}$  values less than or equal to 10-fold than lowest value. Kinases with  $K_d$  or  $IC_{50}$  values ranging from 10-fold to 100-fold, the lowest values are considered tier 2 targets. Each subsequent  $\log_{10}$  increase in  $K_d$  or  $IC_{50}$  comprises a new tier of kinase targets (Fig. 3A; bottom). Next, the  $IC_{50}$  results from an individual patient sample are subdivided into drugs to which the sample was hypersensitive (defined by a patient-specific  $IC_{50}$  that is 5-fold less than the cohort median  $IC_{50}$ ) as well as the drugs to which the sample is not sensitive (Fig. 3B). We next devised a scoring system that assigns points to each kinase based on

whether inhibitors defined to block that kinase target were effective (positive points awarded to the target's score) or ineffective (negative points deducted from the target's score). The addition or subtraction of points is conducted in a graded manner with tier 1 kinases having the most points added or subtracted from their score and the score for kinases from each subsequent tier being modified to lesser degrees (Fig. 3C). Finally, the cumulative scores for each kinase are tabulated and ranked such that the highest scoring kinases for any given patient are those kinases predicted to be most probable in explaining the observed drug response and, therefore, the most probable in playing a pathogenic role for that patient's malignancy (Fig. 3D).

#### Application of oncoprotein prediction algorithm to four proof-of-principle examples

To test this algorithm, we chose 3 specimens from patients with leukemia with known, dysregulated tyrosine kinase pathways and one specimen from a patient without a known kinase mutation. The first example, AML patient 08024, was described in Fig. 3 whereby the FLT3-ITD gene target was predicted on the basis of analysis of the response pattern of the cells to 5

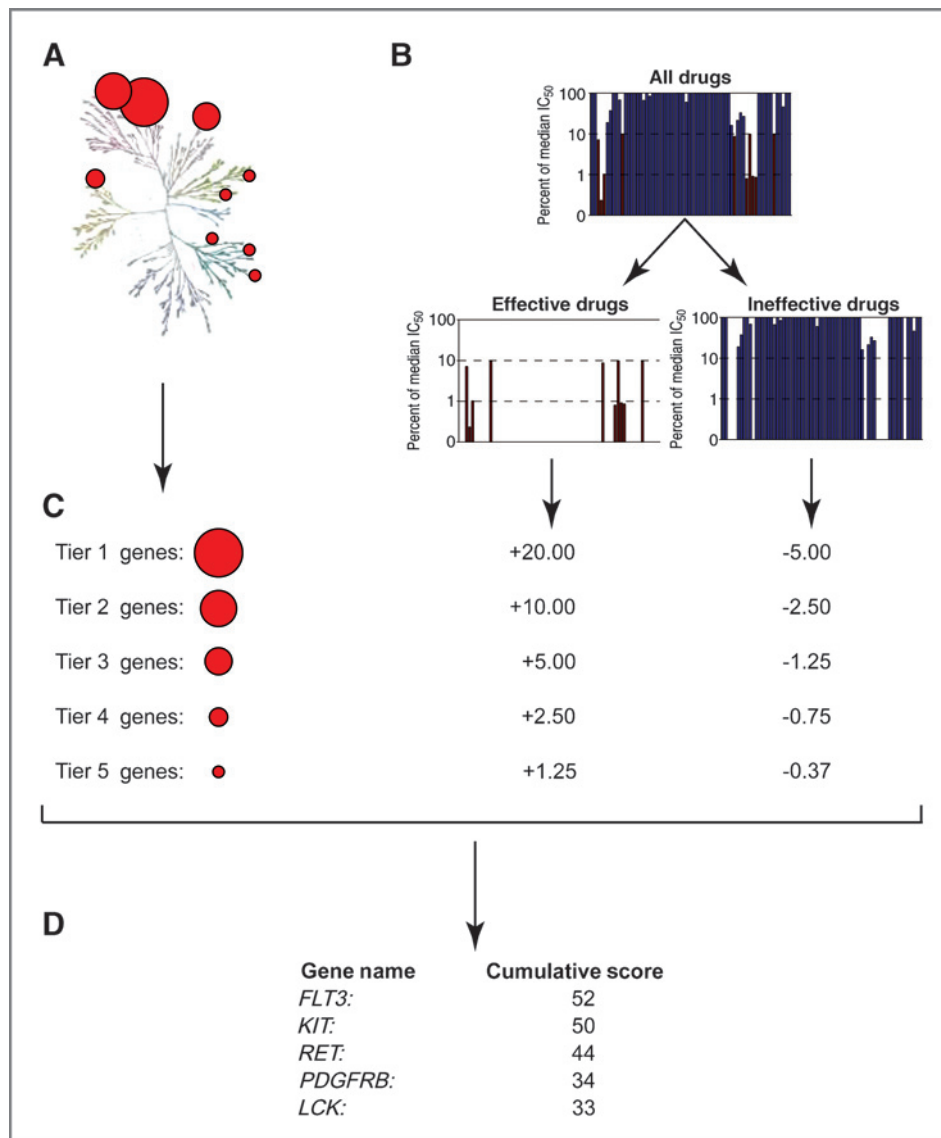


**Figure 3.** Development of an algorithm for kinase target prediction based on kinase inhibitor efficacy. Automation of kinase target prediction based on kinase inhibitor sensitivity patterns proceeds in several steps: **A**, the kinase targets of each kinase inhibitor are curated into a single database from published sources. The kinase target with lowest  $K_d/IC_{50}$  for a given inhibitor as well as all kinase targets with  $K_d/IC_{50}$  less than or equal to 10-fold than lowest value are considered tier 1 targets. Targets with  $K_d/IC_{50}$  within each subsequent 10-fold increase in  $K_d/IC_{50}$  are considered to be in tiers 2 to 5, respectively. Illustration reproduced courtesy of Cell Signaling Technology, Inc. ([www.cellsignal.com](http://www.cellsignal.com)). **B**, drug  $IC_{50}$ s for an individual patient sample are compared with median drug  $IC_{50}$ s to determine effective and ineffective drugs, as described in Fig. 1. **C**, kinase targets of effective drugs are given positive points and kinase targets of ineffective drugs receive negative points, both in a tiered fashion based on the target tiers defined in **A**. **D**, total scores are tabulated for every kinase target and ranked such that targets with the highest points are predicted to be most probable for operational involvement in preservation of cell viability and, therefore, most likely to mechanistically underlie the observed drug sensitivity pattern.

small-molecule kinase inhibitors. To determine whether our algorithm would also successfully identify *FLT3* as a high probability target when applying data from all 66 drugs, we conducted the algorithm on kinase inhibitor panel screening outcomes from this patient sample. This exercise revealed that *FLT3* was the second highest scoring kinase on the target list with a score of 89 points (Fig. 4A). The highest scoring kinase (*EGFR*) scored 90 points due to near complete hypersensitivity of this specimen to ERBB family inhibitors. Analysis of target profiles of these ERBB family inhibitors reveals that they do not exhibit off-target effects against *FLT3* (37), indicating that there may be cross-talk between the *FLT3-ITD* oncogene and ERBB family members. We also applied this screen to cells from a patient with CML in blast crisis. In this case, the algorithm correctly identified *ABL1* as the top-scoring kinase (Fig. 4B). Finally, we applied this technique to cells from a patient with MPN positive for the oncogene, *MPL-W515L*. In this case, 3 of

the top 5 targets are JAK family kinases, which represent therapeutic targets downstream of *MPL* (*MPL* is not a kinase, but signals through JAK kinases; refs. 44, 45; Fig. 4C). Thus, application of this algorithm to 3 proof-of-principle examples shows that the approach correctly identifies known oncogenic signaling pathways in each case. In addition, a patient with AML (08102) with no known mutations in tyrosine kinases exhibited hypersensitivity to 12 of the kinase inhibitors on our panel (Fig. 4D). Among the kinases predicted by our algorithm to be likely involved in pathogenesis of this specimen was *FLT3*, which is commonly mutated in AML (Fig. 4E). However, as noted above, this patient did not exhibit any of the common *FLT3* abnormalities. This prompted us to conduct more extensive sequencing of *FLT3*, and we identified a point mutation in the extracellular region of *FLT3* (S451F; Fig. 4F), this rare mutation has been previously shown to exhibit transformative capacity (46).



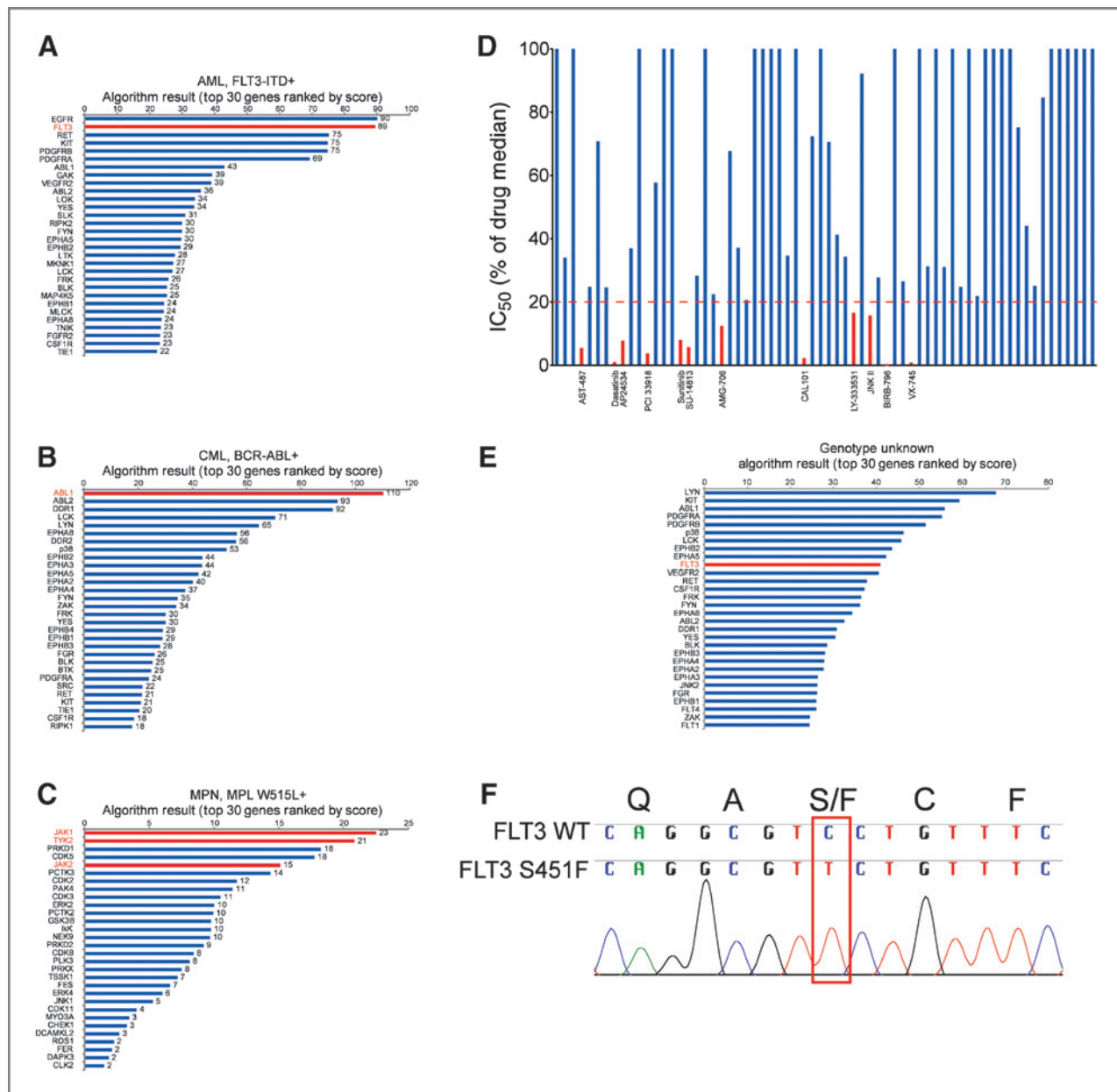
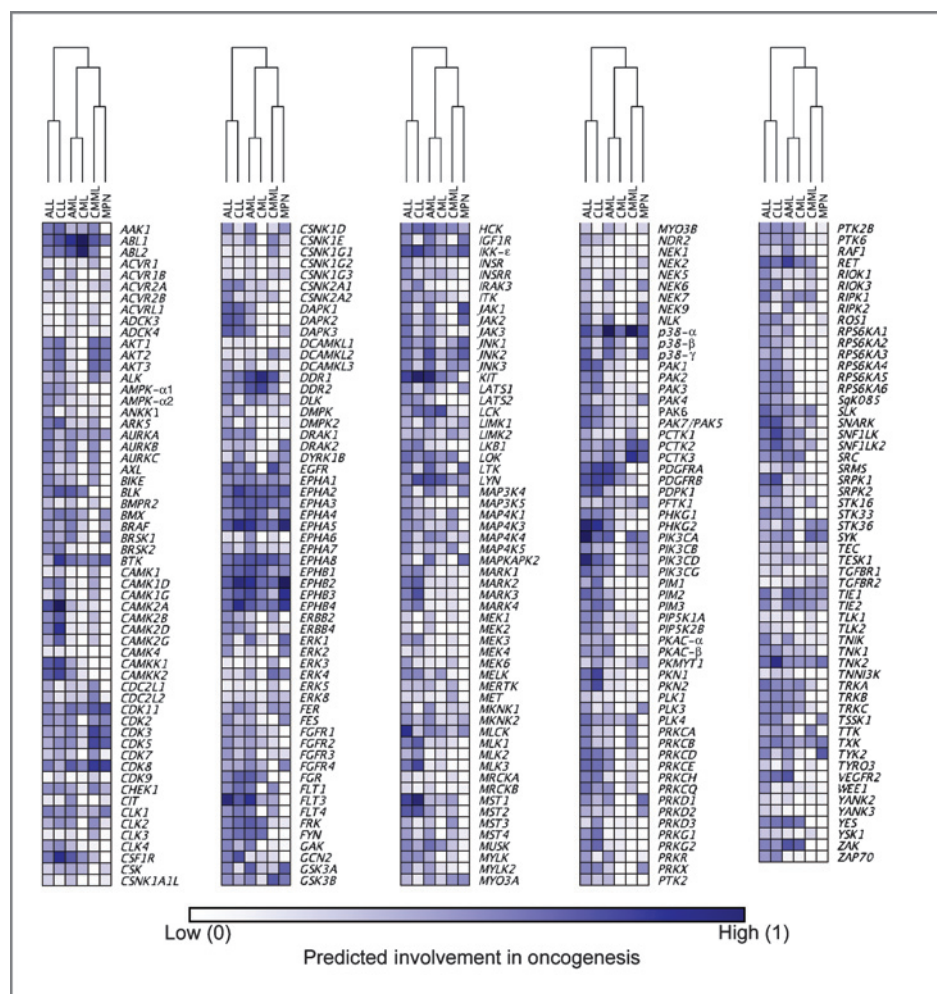


Figure 4. Algorithm kinase target scores for 4 leukemia patient samples with known oncogenic lesions. Proof-of-principle of performance of algorithm described in Fig. 3. The algorithm kinase target scores from 3 patient samples with known genetic etiology are considered. The first sample (A) is an AML patient with *FLT3-ITD*, and FLT3 ranks as the second highest kinase target. EGFR is the highest scoring kinase in this example due to complete hypersensitivity of the specimen to ERBB family inhibitors. This may reveal a mechanistic link between FLT3 and ERBB family signaling, as the ERBB family inhibitors do not exhibit affinity for FLT3. The second sample (B) is derived from a patient with CML in blast crisis with no kinase domain mutations in BCR-ABL. ABL1 is the top scoring kinase for this sample. The third example (C) is an MPN patient with an MPL-W515L mutation. Although MPL is not a kinase (and is not scored by the algorithm), it signals primarily through JAK kinases. Notably, JAK1, JAK2, and TYK2 are 3 of the top 5 scoring kinases for this example. A fourth patient with no known kinase mutations exhibited sensitivity to a variety of kinase inhibitors on our panel (D). The algorithm described in Fig. 3 predicted this pattern to be driven by dependence on a variety of type III receptor tyrosine kinases, including FLT3, which is commonly mutated in AML (E). Because this patient did not exhibit any of the FLT3 mutations commonly observed in AML, we sequenced full-length FLT3 and identified a rare point mutation in the FLT3 extracellular domain (S451F), previously shown to exhibit transformative capacity. The sequence trace of this mutant FLT3 allele is shown in F.

#### Algorithmic prediction of oncogenic signaling pathways in 151 patient samples

To better understand the kinase targets that might underlie drug sensitivity patterns in our entire cohort of leukemia patient samples, we applied our target prediction algorithm to all 151

specimens that were interrogated by the kinase inhibitor panel. The data reveal a heterogeneous list of probable kinase targets that arise in a highly patient-specific manner (Supplementary Table S5). One clear conclusion from these results is the need for a personalized approach to application of kinase-targeted

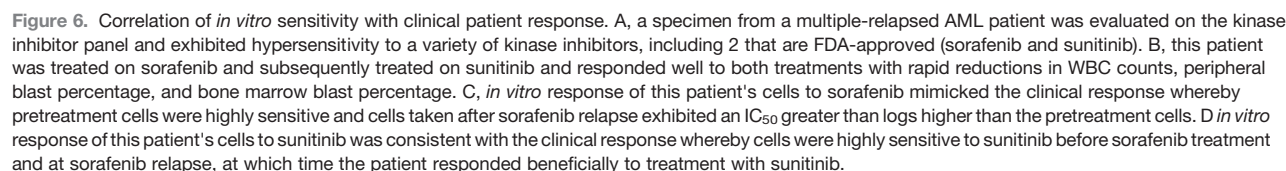


**Figure 5.** Cumulative algorithm kinase target scores by diagnosis. To gain insight into targets that are frequently and infrequently predicted in various diagnostic subsets of leukemia, we tabulated cumulative kinase target scores for ALL, AML, CLL, CML, CMML, and other MPN. Target scores for all 151 patients were tabulated by the algorithm described in Fig. 4 (individual patient target scores can be found in Supplementary Table S5). To compute cumulative scores, all negative values were eliminated and remaining positive values were normalized for each patient to that patient's respective highest scoring kinase, such that all scores were on the same scale from 0 to 1 for every patient. The mean of these normalized scores for each kinase was then calculated for every patient within the above diagnostic leukemia subsets. These average target scores for each leukemia subset were once again normalized to the highest scoring respective gene from within each leukemia subset such that each subset was represented on the same 0 to 1 scale. These values are illustrated on a heatmap where darkest blue indicates targets most frequently predicted to be operationally important within each respective leukemia subset and white indicating no evidence for functional importance. Notably, as a proof-of-principle, ABL1 is the highest cumulative scoring kinase in CML. The numerical input for this heatmap is found in Supplementary Table S6.

therapies. However, the data can also be used to identify kinases that may be more frequently implicated in any one diagnostic subset of malignancy. As such, we tabulated the average kinase scores for each patient within the broad diagnostic categories of ALL, CLL, AML, CML, CMML, and other MPN. Kinase scores were normalized for comparison between patients by dividing all scores of a given profile by the maximum score for that profile. Negative scores were removed resulting in a normalized profile score between 0 and 1. Next, we computed average normalized scores for each kinase across diagnostic groups. Finally, the kinase scores for each diagnostic group were again normalized to the highest scoring kinase within each group so that each diagnostic category would be represented on the same scale. These values were then expressed on a heatmap to visually

represent the kinases that are predicted to be more frequently involved in the pathogenesis of each of these broad diagnostic subsets of hematologic malignancies (Fig. 5; input data found in Supplementary Table S6). As anticipated, ABL1 is the highest cumulative scoring kinase among CML patients tested, serving as a proof-of-principle for this strategy. Interestingly, CaM kinases seem to score highly in lymphoid but not myeloid malignancies. One possible link between that CaM kinases and lymphoid malignancies may be the activation of CBP. Recent studies have identified mutations in CBP (and loss of activity) as a strong correlation with relapse in ALL (47). It has been previously established that phosphorylation of CBP by CaM kinase IV is important for its activity (48). Therefore, inhibition of CaM kinases may provide further insight to the functional





The clinical use of this type of test is predicated on a meaningful correlation between *in vitro* and an *in vivo* response to kinase inhibitors. As a proof-of-concept, we tested this correlation in a patient with refractory AML. A 36 year-old

Downloaded from [cancerres.aacrjournals.org](http://cancerres.aacrjournals.org) on October 9, 2018. © 2013 American Association for Cancer Research.

Treatment with daily sunitinib resulted in a significant initial response with rapid reduction in WBC counts and peripheral leukemic blasts for a period of 4 weeks.

## Discussion

Here, we show that functional screening of primary cells from leukemia patients with a panel of kinase inhibitors can identify effective kinase inhibitors in 70% of patients in just 3 days, including 40% of patient samples that were hypersensitive to drugs already approved for clinical use. We also show an algorithm that uses the partially overlapping kinase target spectra for each drug for prediction of critical kinase targets that underlie inhibitor sensitivity patterns. Finally, using this algorithm, we identify and rank probable kinase targets in 151 patients with a variety of hematologic malignancies.

The predicted kinase targets for these patient samples show a great deal of heterogeneity, even within diagnostic subsets. This finding highlights one of the strengths of this kinase inhibitor screen—kinase targets and patient-specific therapeutic options are detected regardless of the frequency with which these targeted therapies would be applicable within the given disease subset. In addition, although our target prediction algorithm can suggest candidate pathways for follow-up validation, this technique is empirical in that it does not require specific knowledge of any genetic lesion or biomarker to uncover potential therapeutic options for patients.

It is likely that the algorithm shown here exhibits both false-positive and false-negative kinase targets. Because the algorithm is driven by our knowledge of potential target spectra of kinase inhibitors that are present on the panel, there is certainly an opportunity for target bias due to pathways that are over- or under-represented on the panel. As drug development continues and the panel expands to include other drugs that offer more complete and even coverage of the kinome, this pitfall will be diminished. In addition, further profiling of these inhibitors to fully delineate target spectra will also improve the algorithm output as this output is largely driven, and limited, by our knowledge of these target spectra.

It is also possible that the setup of the assay could lead to false-negative results, as the technique relies on a short 3-day window for assessment of drug sensitivity. For this reason, interpretation of negative results from the drug assay (i.e., lack of sensitivity to a particular drug) must be taken with caution. Correlation of results from this screen with clinical cases in which patients are treated with drugs from the panel will help inform the full clinical relevance of both positive and negative assay results.

It will be critical to integrate this kinase inhibitor screen with other cutting edge techniques. We have already begun to apply this assay in conjunction with a related siRNA screen (49, 50), and initial results obtained within 4 days of receiving fresh

primary samples indicate a high concordance of siRNA and kinase inhibitor sensitivities. In addition, application of genomics techniques such as gene expression microarray and deep sequencing in parallel with these functional screening tools will undoubtedly accelerate our understanding of the precise molecular events that underlie the observed kinase sensitivity patterns. Matching of these patient genotypes with drug sensitivity patterns will ultimately enable patients to be treated on the basis of tumor genotypes, and this drug assay and kinase target algorithm offer useful modalities for translation of tumor genotypes into therapeutically relevant clinical strategies. Hence, the kinase inhibitor screen illustrated here represents advancement toward individual patient-tailored cancer therapy. Malignant cells from patients with cancer can be economically screened to identify effective targeted therapies within 3 days, thus matching the appropriate drugs with the appropriate patients on a timescale that affords opportunity for informed, mechanism-based intervention.

## Disclosure of Potential Conflicts of Interest

S.E. Spurgeon has a honoraria from Speakers Bureau from GSK and Millenium. B.J. Druker has ownership interest (including patents) and is a consultant/advisory board member in Blueprint Medicines. No potential conflicts of interest were disclosed by the other authors.

## Authors' Contributions

**Conception and design:** J.W. Tyner, G. Fan, B.H. Chang, M.M. van den Heuvel-Eibrink, B.J. Druker, M.M. Loriaux

**Development of methodology:** J.W. Tyner, G. Fan, M.M. van den Heuvel-Eibrink, T. O'Hare, M.M. Loriaux

**Acquisition of data (provided animals, acquired and managed patients, provided facilities, etc.):** J.W. Tyner, W.F. Yang, L.B. Fletcher, J. Bryant, J.M. Glover, B.H. Chang, S.E. Spurgeon, W.H. Fleming, T. Kovacs, J.R. Gotlib, S.T. Oh, M.W. Deininger, C.M. Zwaan, M.L. den Boer, M.M. van den Heuvel-Eibrink, M.M. Loriaux

**Analysis and interpretation of data (e.g., statistical analysis, biostatistics, computational analysis):** J.W. Tyner, W.F. Yang, A. Bankhead, G. Fan, J.M. Glover, B.H. Chang, W.H. Fleming, C.M. Zwaan, M.L. den Boer, M.M. van den Heuvel-Eibrink, B.J. Druker, M.M. Loriaux

**Writing, review, and/or revision of the manuscript:** J.W. Tyner, G. Fan, B.H. Chang, W.H. Fleming, T. Kovacs, C.M. Zwaan, M.L. den Boer, M.M. van den Heuvel-Eibrink, T. O'Hare, B.J. Druker, M.M. Loriaux

**Administrative, technical, or material support (i.e., reporting or organizing data, constructing databases):** J.W. Tyner, L.B. Fletcher, J.R. Gotlib, M.M. van den Heuvel-Eibrink, M.M. Loriaux

**Study supervision:** J.W. Tyner, M.M. van den Heuvel-Eibrink, B.J. Druker, M.M. Loriaux

## Grant Support

This work was supported in part by The Leukemia and Lymphoma Society, the TJ Martell Foundation, and the Doris Duke Charitable Foundation. J.W. Tyner is supported by grants from the National Cancer Institute (NCI; grant # 5K99CA151457-02) as well as grants from the William Lawrence and Blanche Hughes Foundation and the Oregon Clinical and Translational Research Institute (OCTRI) grant number UL1 RR024140 from the National Center for Research Resources (NRCC), a component of the NIH, and NIH Roadmap for Medical Research. B.J. Druker is an investigator of the Howard Hughes Medical Institute.

The costs of publication of this article were defrayed in part by the payment of page charges. This article must therefore be hereby marked *advertisement* in accordance with 18 U.S.C. Section 1734 solely to indicate this fact.

Received May 18, 2012; revised August 24, 2012; accepted September 13, 2012; published OnlineFirst October 18, 2012.

## References

1. Druker BJ, Guilhot F, O'Brien SG, Gathmann I, Kantarjian H, Gattermann N, et al. Five-year follow-up of patients receiving imatinib for chronic myeloid leukemia. *N Engl J Med* 2006;355:2408-17.
2. Lynch TJ, Bell DW, Sordella R, Gurubhagavatula S, Okimoto RA, Brannigan BW, et al. Activating mutations in the epidermal growth factor receptor underlying responsiveness of non-small-cell lung cancer to gefitinib. *N Engl J Med* 2004;350:2129-39.

3. Paez JG, Jänne PA, Lee JC, Tracy S, Greulich H, Gabriel S, et al. EGFR mutations in lung cancer: correlation with clinical response to gefitinib therapy. *Science* 2004;304:1497–500.
4. Smith I, Procter M, Gelber RD, Guillaume S, Feyereislova A, Dowsett M, et al. 2-year follow-up of trastuzumab after adjuvant chemotherapy in HER2-positive breast cancer: a randomised controlled trial. *Lancet* 2007;369:29–36.
5. Krause DS, Van Etten RA. Tyrosine kinases as targets for cancer therapy. *N Engl J Med* 2005;353:172–87.
6. Paul MK, Mukhopadhyay AK. Tyrosine kinase - role and significance in cancer. *Int J Med Sci* 2004;1:101–15.
7. Shtivelman E, Lifshitz B, Gale RP, Canaani E. Fused transcript of *abl* and *bcr* genes in chronic myelogenous leukaemia. *Nature* 1985;315:550–4.
8. Gunby RH, Cazzaniga G, Tassi E, Le Coutre P, Pogliani E, Specchia G, et al. Sensitivity to imatinib but low frequency of the TEL/PDGFRbeta fusion protein in chronic myelomonocytic leukemia. *Haematologica* 2003;88:408–15.
9. Levine RL, Loriaux M, Huntly BJ, Loh ML, Beran M, Stoffregen E, et al. The JAK2V617F activating mutation occurs in chronic myelomonocytic leukemia and acute myeloid leukemia, but not in acute lymphoblastic leukemia or chronic lymphocytic leukemia. *Blood* 2005;106:3377–9.
10. Lorenzo F, Nishii K, Monma F, Kuwagata S, Usui E, Shiku H. Mutational analysis of the KIT gene in myelodysplastic syndrome (MDS) and MDS-derived leukemia. *Leuk Res* 2006;30:1235–9.
11. Padua RA, Guinn BA, Al-Sabab AI, Smith M, Taylor C, Pettersson T, et al. RAS, FMS and p53 mutations and poor clinical outcome in myelodysplasias: a 10-year follow-up. *Leukemia* 1998;12:887–92.
12. Baxter EJ, Scott LM, Campbell PJ, East C, Fourouclas N, Swanton S, et al. Acquired mutation of the tyrosine kinase JAK2 in human myeloproliferative disorders. *Lancet* 2005;365:1054–61.
13. James C, Ugo V, Le Couëdic JP, Staerk J, Delhommeau F, Lacout C, et al. A unique clonal JAK2 mutation leading to constitutive signalling causes polycythaemia vera. *Nature* 2005;434:1144–8.
14. Kralovics R, Passamonti F, Buser AS, Teo SS, Tiedt R, Passweg JR, et al. A gain-of-function mutation of JAK2 in myeloproliferative disorders. *N Engl J Med* 2005;352:1779–90.
15. Levine RL, Wadleigh M, Cools J, Ebert BL, Wernig G, Huntly BJ, et al. Activating mutation in the tyrosine kinase JAK2 in polycythemia vera, essential thrombocythemia, and myeloid metaplasia with myelofibrosis. *Cancer Cell* 2005;7:387–97.
16. Golub TR, Barker GF, Lovett M, Gilliland DG. Fusion of PDGF receptor beta to a novel ets-like gene, *tel*, in chronic myelomonocytic leukemia with t(5;12) chromosomal translocation. *Cell* 1994;77:307–16.
17. Walters DK, Mercher T, Gu TL, O'Hare T, Tyner JW, Loriaux M, et al. Activating alleles of JAK3 in acute megakaryoblastic leukemia. *Cancer Cell* 2006;10:65–75.
18. Xiang Z, Zhao Y, Mitaksov V, Fremont DH, Kasai Y, Molitoris A, et al. Identification of somatic JAK1 mutations in patients with acute myeloid leukemia. *Blood* 2008;111:4809–12.
19. Yamamoto Y, Kiyoi H, Nakano Y, Suzuki R, Kadera Y, Miyawaki S, et al. Activating mutation of D835 within the activation loop of FLT3 in human hematologic malignancies. *Blood* 2001;97:2434–9.
20. Yokota S, Kiyoi H, Nakao M, Iwai T, Misawa S, Okuda T, et al. Internal tandem duplication of the FLT3 gene is preferentially seen in acute myeloid leukemia and myelodysplastic syndrome among various hematological malignancies. A study on a large series of patients and cell lines. *Leukemia* 1997;11:1605–9.
21. Armstrong SA, Mabon ME, Silverman LB, Li A, Gribben JG, Fox EA, et al. FLT3 mutations in childhood acute lymphoblastic leukemia. *Blood* 2004;103:3544–6.
22. Bercovich D, Ganmore I, Scott LM, Wainreb G, Birger Y, Elimelech A, et al. Mutations of JAK2 in acute lymphoblastic leukaemias associated with Down's syndrome. *Lancet* 2008;372:1484–92.
23. Clark SS, McLaughlin J, Crist WM, Champlin R, Witte ON. Unique forms of the *abl* tyrosine kinase distinguish Ph1-positive CML from Ph1-positive ALL. *Science* 1987;235:85–8.
24. Gaikwad A, Rye CL, Devidas M, Heerema NA, Carroll AJ, Izraeli S, et al. Prevalence and clinical correlates of JAK2 mutations in Down syndrome acute lymphoblastic leukaemia. *Br J Haematol* 2009;144:930–2.
25. Kearney L, Gonzalez De Castro D, Yeung J, Procter J, Horsley SW, Eguchi-Ishimae M, et al. Specific JAK2 mutation (JAK2R683) and multiple gene deletions in Down syndrome acute lymphoblastic leukemia. *Blood* 2009;113:646–8.
26. Mullighan CG, Zhang J, Harvey RC, Collins-Underwood JR, Schulman BA, Phillips LA, et al. JAK mutations in high-risk childhood acute lymphoblastic leukemia. *Proc Natl Acad Sci U S A* 2009;106:9414–8.
27. Fukuda T, Chen L, Endo T, Tang L, Lu D, Castro JE, et al. Antisera induced by infusions of autologous Ad-CD154-leukemia B cells identify ROR1 as an oncofetal antigen and receptor for Wnt5a. *Proc Natl Acad Sci U S A* 2008;105:3047–52.
28. Chen L, Widhopf G, Huynh L, Rassenti L, Rai KR, Weiss A, et al. Expression of ZAP-70 is associated with increased B-cell receptor signaling in chronic lymphocytic leukemia. *Blood* 2002;100:4609–14.
29. Contri A, Brunati AM, Trentin L, Cabrelle A, Miorin M, Cesaro L, et al. Chronic lymphocytic leukemia B cells contain anomalous Lyn tyrosine kinase, a putative contribution to defective apoptosis. *J Clin Invest* 2005;115:369–78.
30. McCaig AM, Cosimo E, Leach MT, Michie AM. Dasatinib inhibits B cell receptor signalling in chronic lymphocytic leukaemia but novel combination approaches are required to overcome additional pro-survival microenvironmental signals. *Br J Haematol* 2011;153:199–211.
31. Greenman C, Stephens P, Smith R, Dalgleish GL, Hunter C, Bignell G, et al. Patterns of somatic mutation in human cancer genomes. *Nature* 2007;446:153–8.
32. Loriaux MM, Levine RL, Tyner JW, Fröhling S, Scholl C, Stoffregen EP, et al. High-throughput sequence analysis of the tyrosine kinase in acute myeloid leukemia. *Blood* 2008;111:4788–96.
33. Sjöblom T, Jones S, Wood LD, Parsons DW, Lin J, Barber TD, et al. The consensus coding sequences of human breast and colorectal cancers. *Science* 2006;314:268–74.
34. Tomasson MH, Xiang Z, Walgren R, Zhao Y, Kasai Y, Miner T, et al. Somatic mutations and germline sequence variants in the expressed tyrosine kinase genes of patients with *de novo* acute myeloid leukemia. *Blood* 2008;111:4797–808.
35. Fabian MA, Biggs WH, Treiber DK, Atteridge CE, Azimioara MD, Benedetti MG, et al. A small molecule-kinase interaction map for clinical kinase inhibitors. *Nat Biotechnol* 2005;23:329–36.
36. Hantschel O, Rix U, Schmidt U, Bürckstümmer T, Knedinger M, Schütze G, et al. The Btk tyrosine kinase is a major target of the Bcr-Abl inhibitor dasatinib. *Proc Natl Acad Sci U S A* 2007;104:13283–8.
37. Karaman MW, Herrgard S, Treiber DK, Gallant P, Atteridge CE, Campbell BT, et al. A quantitative analysis of kinase inhibitor selectivity. *Nat Biotechnol* 2008;26:127–32.
38. Zarrinkar PP, Gunawardane RN, Cramer MD, Gardner MF, Brigham D, Belli B, et al. AC220 is a uniquely potent and selective inhibitor of FLT3 for the treatment of acute myeloid leukemia (AML). *Blood* 2009;114:2984–92.
39. Lannutti BJ, Meadows SA, Herman SE, Kashishian A, Steiner B, Johnson AJ, et al. CAL-101, a p110delta selective phosphatidylinositol-3-kinase inhibitor for the treatment of B-cell malignancies, inhibits PI3K signaling and cellular viability. *Blood* 2011;117:591–4.
40. O'Hare T, Shakespeare WC, Zhu X, Eide CA, Rivera VM, Wang F, et al. AP24534, a pan-BCR-ABL inhibitor for chronic myeloid leukemia, potently inhibits the T315I mutant and overcomes mutation-based resistance. *Cancer Cell* 2009;16:401–12.
41. Tyner JW, Bumm TG, Deininger J, Wood L, Aichberger KJ, Loriaux MM, et al. CYT387, a novel JAK2 inhibitor, induces hematologic responses and normalizes inflammatory cytokines in murine myeloproliferative neoplasms. *Blood* 2010;115:5232–40.
42. Honigberg LA, Smith AM, Sirisawad M, Verner E, Lory D, Chang B, et al. The Bruton tyrosine kinase inhibitor PCI-32765 blocks B-cell activation and is efficacious in models of autoimmune disease and B-cell malignancy. *Proc Natl Acad Sci U S A* 2010;107:13075–80.
43. Pan Z, Scheerens H, Li SJ, Schultz BE, Sprengeler PA, Burrill LC, et al. Discovery of selective irreversible inhibitors for Bruton's tyrosine kinase. *ChemMedChem* 2007;2:58–61.
44. Pikman Y, Lee BH, Mercher T, McDowell E, Ebert BL, Gozo M, et al. MPLW515L is a novel somatic activating mutation in myelofibrosis with myeloid metaplasia. *PLoS Med* 2006;3:e270.



45. Sattler M, Durstin MA, Frank DA, Okuda K, Kaushansky K, Salgia R, et al. The thrombopoietin receptor c-MPL activates JAK2 and TYK2 tyrosine kinases. *Exp Hematol* 1995;23:1040–8.
46. Frohling S, Scholl C, Levine RL, Loriaux M, Boggon TJ, Bernard OA, et al. Identification of driver and passenger mutations of FLT3 by high-throughput DNA sequence analysis and functional assessment of candidate alleles. *Cancer Cell* 2007;12:501–13.
47. Mullighan CG, Zhang J, Kasper LH, Lerach S, Payne-Turner D, Phillips LA, et al. CREBBP mutations in relapsed acute lymphoblastic leukaemia. *Nature* 2011;471:235–9.
48. Impey S, Fong AL, Wang Y, Cardinaux JR, Fass DM, Obrietan K, et al. Phosphorylation of CBP mediates transcriptional activation by neural activity and CaM kinase IV. *Neuron* 2002;34:235–44.
49. Tyner JW, Deininger MW, Loriaux MM, Chang BH, Gotlib JR, Willis SG, et al. RNAi screen for rapid therapeutic target identification in leukemia patients. *Proc Natl Acad Sci U S A* 2009;106:8695–700.
50. Tyner JW, Walters DK, Willis SG, Luttropp M, Oost J, Loriaux M, et al. RNAi screening of the tyrosine kinome identifies therapeutic targets in acute myeloid leukemia. *Blood* 2008;111:2238–45.

# Cancer Research

The Journal of Cancer Research (1916–1930) | The American Journal of Cancer (1931–1940)

## Kinase Pathway Dependence in Primary Human Leukemias Determined by Rapid Inhibitor Screening

Jeffrey W. Tyner, Wayne F. Yang, Armand Bankhead III, et al.

*Cancer Res* 2013;73:285-296. Published OnlineFirst October 18, 2012.

<b>Updated version</b>	Access the most recent version of this article at: doi: <a href="https://doi.org/10.1158/0008-5472.CAN-12-1906">10.1158/0008-5472.CAN-12-1906</a>
<b>Supplementary Material</b>	Access the most recent supplemental material at: <a href="http://cancerres.aacrjournals.org/content/suppl/2012/10/18/0008-5472.CAN-12-1906.DC1">http://cancerres.aacrjournals.org/content/suppl/2012/10/18/0008-5472.CAN-12-1906.DC1</a>

<b>Cited articles</b>	This article cites 50 articles, 21 of which you can access for free at: <a href="http://cancerres.aacrjournals.org/content/73/1/285.full#ref-list-1">http://cancerres.aacrjournals.org/content/73/1/285.full#ref-list-1</a>
<b>Citing articles</b>	This article has been cited by 24 HighWire-hosted articles. Access the articles at: <a href="http://cancerres.aacrjournals.org/content/73/1/285.full#related-urls">http://cancerres.aacrjournals.org/content/73/1/285.full#related-urls</a>

<b>E-mail alerts</b>	<a href="#">Sign up to receive free email-alerts</a> related to this article or journal.
<b>Reprints and Subscriptions</b>	To order reprints of this article or to subscribe to the journal, contact the AACR Publications Department at <a href="mailto:pubs@aacr.org">pubs@aacr.org</a> .
<b>Permissions</b>	To request permission to re-use all or part of this article, use this link <a href="http://cancerres.aacrjournals.org/content/73/1/285">http://cancerres.aacrjournals.org/content/73/1/285</a> . Click on "Request Permissions" which will take you to the Copyright Clearance Center's (CCC) Rightslink site.